Dalton Transactions

Accepted Manuscript

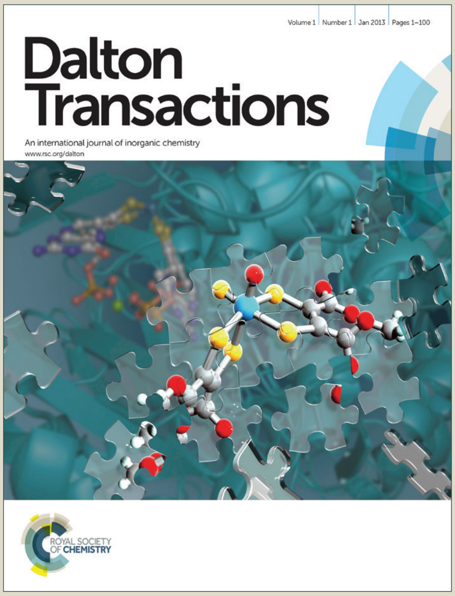

ROYAL SOCIETY OF CHEMISTRY

www.rsc.org/dalton

Journal Name

RSCPublishing

ARTICLE

An unusual density evolution between $SrCdB_2O_5$ polymorphs

Cite this: DOI: 10.1039/x0xx00000x

Xingwen Zhang,[a,b] Zhengyang Zhou,[c] Hongping Wu,[*a] Shilie Pan,[*a] Chen Lei,[a,b] Lu Liu,[a,b] and Zhihua Yang[a]

Received 00th January 2012,
Accepted 00th January 2012

DOI: 10.1039/x0xx00000x

www.rsc.org/

Owing to the effect of atomic vibrations, high-temperature phase usually features a relatively smaller density when compared with low-temperature phase. In this work, a new $SrCdB_2O_5$ phase has been discovered. According to the crystallization temperature from low to high, the new $SrCdB_2O_5$ phase can be regarded as the high-temperature β-$SrCdB_2O_5$ phase. The density of β-$SrCdB_2O_5$ is obviously larger than that of α-$SrCdB_2O_5$, meanwhile β-$SrCdB_2O_5$ is energy favored. This unusual density evolution phenomenon has been investigated. In addition, the Pb^{2+}-doped compounds, $Pb_xSr_{1-x}CdB_2O_5$ (x = 0.125, 0.25, 0.375, 0.5), have also been investigated by powder refinement.

Introduction

Polymorphism has long been the subject of interest over many decades not only because of its important applications in pharmaceuticals, pigments, foods, dyestuffs and so forth, but also for investigating the crystallization process, particular for the research of structure-property relationship.[1-3] Recently, considerable attention about polymorphism has been focused on borates because of their rich structural chemistry and many borate polymorphs with high practical value have been systematically investigated, such as α- and β-BaB_2O_4.[4-5] Generally, the high-temperature phase (β-phase) usually features a smaller density than the low-temperature phase (α-phase) due to the inherent anharmonicity of bond vibrations. Certainly, in some rare examples, the β-phase may characterize a nearly density value with the α-phase, such as α-$Li_4B_2O_5$ (ρ: 2.033 Mg/m^3) and β-$Li_4B_2O_5$ (ρ: 2.039 Mg/m^3).[6] However, in our exploration of borate polymorphism, $SrCdB_2O_5$ represents a very puzzling case that the density of α- and β-$SrCdB_2O_5$ are 4.571 and 4.688 Mg/m^3 in room temperature, respectively, revealing that the density of the high-temperature phase is obviously larger than that of the low-temperature one. Moreover, β-$SrCdB_2O_5$ crystallizes in a monoclinic unit cell while α-$SrCdB_2O_5$ is orthorhombic, which is also unusual, because a compound usually will lose symmetry elements undergoing a phase transition from high temperature to low temperature.

In this work, from the structure chemistry point of view, we analyzed their similar crystal structures of α- and β-$SrCdB_2O_5$, and finally discovered the underlying reasons of the unusual density phenomenon. Furthermore, to gain insight into the phase transformation of $SrCdB_2O_5$, polycrystalline samples of *β*-$SrCdB_2O_5$ were synthesized by traditional solid-state reaction techniques at different reaction temperatures and TG-DSC measurement of α-$SrCdB_2O_5$ was also carried out. A new $Cd_2B_2O_5$ phase was obtained by quenched experiment. Besides, the total electronic energy of α- and β-$SrCdB_2O_5$ based on experimental crystallographic data were also been calculated and according to the data, the low-temperature phase, namely α-$SrCdB_2O_5$, is metastable when compared with β-$SrCdB_2O_5$. For confirming this viewpoint, we also substituted the Sr^{2+} cation for Pb^{2+} successfully to form $Pb_{0.125}Sr_{0.875}CdB_2O_5$, $Pb_{0.25}Sr_{0.75}CdB_2O_5$, $Pb_{0.375}Sr_{0.625}CdB_2O_5$ and $Pb_{0.5}Sr_{0.5}CdB_2O_5$. The corresponding powder X-ray diffraction (XRD) patterns suggest that the Pb^{2+}-doped compounds, $Pb_xSr_{1-x}CdB_2O_5$ (x = 0.125, 0.25, 0.375, 0.5), adopt the similar structure type of *β*-$SrCdB_2O_5$, consistent with the calculation result that *β*-$SrCdB_2O_5$ is energy favored. We also carried out some related measurements, such as IR spectrum and UV-Vis-NIR diffuse reflectance spectrum for *β*-$SrCdB_2O_5$, and some theoretical calculations, such as band structure and densities of states for *β*-$SrCdB_2O_5$. In this paper, we mainly report an unusual density and crystal symmetry behavior of $SrCdB_2O_5$. To proceed from this point, we did some related interesting researches.

Experimental

Reagents

$Sr(NO_3)_2$ (99.0%, Sinopharm Chemical Reagent Co., Ltd.), CdO (99.0%, Tianjin Bodi Chemical Co., Ltd.), PbO (99.0%, Sinopharm Chemical Reagent Co., Ltd.) and H_3BO_3 (Tianjin Baishi Chemical Co., Ltd., 99.5%) were used as received.

Crystal Growth

Small single crystals of *α*- and *β*-$SrCdB_2O_5$ were grown from a high-temperature solution with flux systems in air. A mixture of raw materials $Sr(NO_3)_2$-CdO-H_3BO_3-PbO with molar ratio (1 : 1 : 5 : 3 for *α*-$SrCdB_2O_5$, 1 : 1 : 4 : 2 for *β*-$SrCdB_2O_5$) was loaded in a Pt crucible and heated in a muffle furnace at 900 ℃ until the solution became transparent and clear. The homogenized solution was then cooled quickly (20 ℃/h) to the crystallization temperature (750 ℃ for *α*-$SrCdB_2O_5$, 780 ℃ for *β*-$SrCdB_2O_5$), then slowly cooled (3 ℃/h) to (700 ℃ for *α*-$SrCdB_2O_5$, 730 ℃ for *β*-$SrCdB_2O_5$) followed by cooling to room temperature after the furnace was powered off. Small colorless crystals of *α*- and *β*-$SrCdB_2O_5$ were obtained for the structure determination.

X-ray Crystallography

The single crystals of α- and β-$SrCdB_2O_5$ were selected and mounted on thin glass fibers of the Bruker SMART APEX II CCD diffractometer. Data were collected using monochromatic Mo Kα radiation (λ = 0.71073 Å) at 296(2) K and integrated with the SAINT program.[7] All calculations were performed with programs from the SHELXTL crystallographic software package.[8] The structures were solved by direct methods using SHELXS-97.[9] The final full-matrix least-squares refinement were on F_o^2 with data having $F_o^2 \geq 2\sigma(F_o^2)$ and all of the atoms were refined with anisotropic thermal parameters. The structures of α- and β-$SrCdB_2O_5$ were checked for missing symmetry elements with *PLATON*.[10] The crystal data and structure refinement are presented in Table 1. The atomic coordinates, related anisotropic displacement parameters, the bond valence calculations[11] for all atoms and selected bond lengths (Å) and angles (deg.) are summarized in Tables S1−S3 in the SI.

Table 1. Crystal data and structure refinement for $Pb_{0.4}Sr_{0.6}CdB_2O_5$, α- and β-$SrCdB_2O_5$.

Formula	α-$SrCdB_2O_5$	β-$SrCdB_2O_5$	$Pb_{0.4}Sr_{0.6}CdB_2O_5$
fw	301.64	301.64	349.48
Crystal system	Orthorhombic	Monoclinic	Monoclinic
Space group	*Pbca*	*C2/c*	*C2/c*
Z	8	8	8
a (Å)	11.9454(19)	7.6343(8)	7.597(14)
b (Å)	5.7798(9)	10.1827(10)	10.280(18)
c (Å)	12.698(2)	11.1385(12)	11.28(2)
β (deg)	90	99.228(7)	98.96(2)
V (Å^3)	876.7(2)	854.68(15)	870(3)
ρ (calcd) (Mg/m^3)	4.571	4.688	5.289
F(000)	1088	1088	1220
μ (mm^{-1})	16.933	17.369	17.023
θ (deg.)	3.21-35.08	3.36-34.97	3.36-27.45
Index range	$-19 \leq h \leq 19$ $-9 \leq k \leq 9$ $-19 \leq l \leq 20$	$-11 \leq h \leq 12$ $-16 \leq k \leq 16$ $-17 \leq l \leq 17$	$-9 \leq h \leq 9$ $-12 \leq k \leq 13$ $-14 \leq l \leq 10$
R_{int}	0.0703	0.0564	0.0394
Completeness to θ	99.1 %	99.2 %	98.7 %
R_1/wR_2 (I > 2σ (I))[a]	0.0366/0.0995	0.0268/0.0478	0.0249/ 0.0512
R_1/wR_2 (all data)[a]	0.0553/0.1077	0.0436/0.0521	0.0283/ 0.0526
GOF on F^2	1.131	1.045	1.048
Largest diff. peak and hole (e ·Å^{-3})	2.864 and -2.654	1.374 and -1.016	1.167 and -1.158

[a] $R_1 = \Sigma||F_o| - |F_c||/\Sigma|F_o|$ and $wR_2 = [\Sigma w(F_o^2 - F_c^2)^2 / \Sigma w F_o^4]^{1/2}$ for $F_o^2 > 2\sigma(F_o^2)$

Powder X-ray Diffraction

Powder X-ray diffraction (XRD) analysis of α- and β-$SrCdB_2O_5$ were performed at room temperature in the angular range of 10° < 2θ < 70° with a scan step width of 0.02° and fixed counting time of 1 s/step with a Bruker D2 PHASER diffractometer equipped with a diffracted beam monochromator set for Cu Kα radiation (λ = 1.5418 Å). Powder XRD data of $Pb_xSr_{1-x}CdB_2O_5$ (x = 0.125, 0.25, 0.375, 0.5) were also obtained at room temperature using the Bruker D2 PHASER diffractometer equipped with a diffracted beam monochromator set for Cu Kα radiation (λ = 1.5418 Å). The powder XRD patterns were analyzed using the Rietveld method with the Jana2006 program.[12] The structural refinements of the solid solutions were performed in the space group *C2/c* (No. 15) with a starting model using the single crystal data of β-$SrCdB_2O_5$. We did not observe any crystallographic ordering between the Pb^{2+} and Sr^{2+} cations. Therefore, for $Pb_xSr_{1-x}CdB_2O_5$ (x = 0.125, 0.25, 0.375, 0.5), the Pb^{2+} and Sr^{2+} were statistically disordered over the two unique Sr^{2+} sites in β-$SrCdB_2O_5$. By doing so, the resulting formulae are in good agreement with the stoichiometry (see the Powder XRD patterns). The crystallographic data and refinement results for $Pb_xSr_{1-x}CdB_2O_5$ (x = 0.125, 0.25, 0.375, 0.5) are summarized in Table 2.

Thermal Analysis

Thermal analysis of α-$SrCdB_2O_5$ was carried out on a simultaneous NETZSCH STA 449C thermal analyzer instrument with a heating rate of 5 ℃/min. The measurement range extended from 35 to 1000 ℃ in an atmosphere of flowing N_2.

IR Spectroscopy

The IR absorption spectrum was recorded on a Shimadzu IR Affinity-1 Fourier transform IR spectrometer to analyze the presence of functional groups in β-$SrCdB_2O_5$. The sample was mixed thoroughly with dried KBr (1 mg of the sample, 100 mg of KBr). The spectrum was collected in the range from 400 to 4000 cm^{-1} with a resolution of 2 cm^{-1}.

UV-Vis-NIR Diffuse Reflectance Spectrum

UV-Vis-NIR diffuse reflectance spectrum of β-$SrCdB_2O_5$ was measured at room temperature with a Shimadzu SolidSpec-3700DUV spectrophotometer. Data were collected in the wavelength range 190–2600 nm. And the reflectance spectrum was converted to absorbance with the Kubelka−Munk function.[13]

Numerical Calculation Details

The electronic structure of β-$SrCdB_2O_5$ was calculated using the *ab initio* density functional theory (DFT) method implemented in the CASTEP package.[14] The Perdew-Burke-Emzerhoff (PBE) functional within the generalized gradient approximation (GGA) was employed for exchange-correlation potential.[15] Plane-wave cutoff for a norm-conserving pseudopotential is 750 eV. The Monkhorst–Pack grid[16] was set by 2 × 2 × 1 in the Brillouinzone of the unit cell. Norm-conserving pseudopotentials (NCP) was employed.[17]

Results and discussion

Crystals of α- and β-$SrCdB_2O_5$ were synthesized by spontaneous crystallization with the flux method in the SrO-CdO–B_2O_3 system. Their crystal data and structure refinement are listed in Table 1. α-$SrCdB_2O_5$ has been reported before.[18] α- and β-$SrCdB_2O_5$ crystallize in orthorhombic space group *Pbca* and monoclinic space group *C*2/*c*, respectively. Both of them can be described as different Sr-O layers that stack one over another and the Cd and B atoms are located between adjacent layers, forming the final crystal structures, as shown in Figure S1 in the SI. Detailedly, both of the α- and β-$SrCdB_2O_5$ structures are built up of SrO_8, CdO_6 and isolated B_2O_5 groups. The theoretical density of α- and β-$SrCdB_2O_5$ are 4.571 and 4.688 Mg/m^3, respectively. The experimental density which were measured by pycnometer method are 4.2(1) and 4.5(1) Mg/m^3, respectively. In spite of a obvious difference between experimental value and theoretical value, the measurement result still can prove that the density of β-$SrCdB_2O_5$ is larger than that of α-$SrCdB_2O_5$. In order to investigate the unusual density phenomenon, we should pay particular attention to the structure chemistry of α- and β-$SrCdB_2O_5$

to find their similarity, difference and relationship. Firstly, the isolated B_2O_5 groups in them have different dihedral angles (59.4(2) ° in α-$SrCdB_2O_5$ and 42.7(2) ° in β-$SrCdB_2O_5$), as shown in Figure 1. Meanwhile, the distortions of SrO_8 and CdO_6 polyhedra in α- and β-$SrCdB_2O_5$ are distinct revealed by the magnitudes of dipole moments (Table S4 in the SI). Furthermore, the most significant difference between α- and β-$SrCdB_2O_5$ is the Sr-O layer, as shown in Figure 2. There are four-membered $[Sr_4O_4]$ rings on *ac* plane in α-$SrCdB_2O_5$ while six-membered $[Sr_6O_6]$ rings in β-$SrCdB_2O_5$, as shown in Figure 3. However, though the [Sr-O] rings are different between them, the $[Sr_6O_6]$ rings in β-$SrCdB_2O_5$ could be derived from the $[Sr_4O_4]$ rings in α-$SrCdB_2O_5$ by splitting the O5 atoms into two oxygen atoms. Moreover, the Sr-O layer is planar in β-$SrCdB_2O_5$ while buckled in α-$SrCdB_2O_5$, as shown in Figure 2. We deem that the different dihedral angles of B_2O_5 groups in α- and β-$SrCdB_2O_5$ result in different Sr-O layers and crystal structures. As shown in Figure 2, the distance between the Sr-O layers in α-$SrCdB_2O_5$ (6.329 Å) is longer than that in β-$SrCdB_2O_5$ (5.497 Å). This is the direct reason why α-$SrCdB_2O_5$ possesses a smaller density than β-$SrCdB_2O_5$.

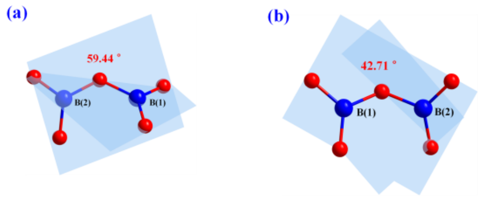

Figure 1. The isolated B_2O_5 groups in α-$SrCdB_2O_5$ (a) and β-$SrCdB_2O_5$ (b).

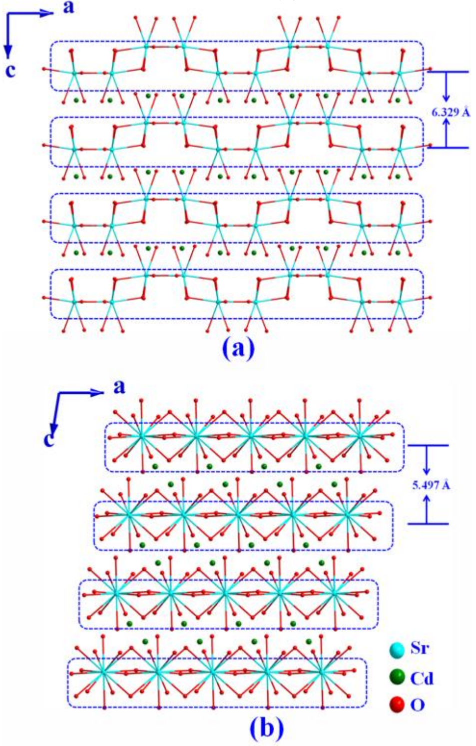

Figure 2. The structures of (a) α-$SrCdB_2O_5$ and (b) β-$SrCdB_2O_5$. The boron atoms are removed for clarity.

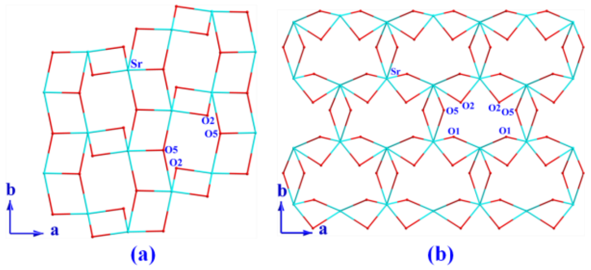

Figure 3. The Sr-O layer in (a) α-$SrCdB_2O_5$ and (b) β-$SrCdB_2O_5$. The terminal oxygen atoms are removed for clarity.

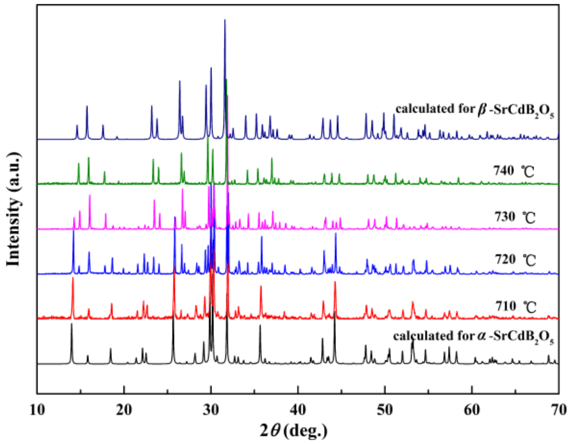

Figure 4. Powder XRD patterns showing the influence of reaction temperature on polymorph transformation of $SrCdB_2O_5$.

Table 2. Summary of the crystallographic data and refinement results for $Pb_xSr_{1-x}CdB_2O_5$ (x = 0.125, 0.25, 0.375, 0.5).

x	x = 0.125	x = 0.25	x = 0.375	x = 0.5
fw	316.59	331.55	346.49	361.44
Space group	*C*2/*c*	*C*2/*c*	*C*2/*c*	*C*2/*c*
a (Å)	7.61871(14)	7.59760(16)	7.57839(16)	7.5552(3)
b (Å)	10.1893(2)	10.2002(2)	10.2213(2)	10.2370(5)
c (Å)	11.1634(2)	11.1885(2)	11.2313(3)	11.2710(5)
β (deg)	99.1688(11)	99.1163(12)	99.1016(12)	99.0988(14)
V ($Å^3$)	855.53(3)	856.13(3)	859.04(3)	860.76(7)
R_p	0.0332	0.0303	0.0367	0.0308
Rw_p	0.0452	0.0424	0.0479	0.0435

To gain insight into the phase transition of $SrCdB_2O_5$, the following experiments and measurements were carried out. (1) Polycrystalline samples of β-$SrCdB_2O_5$ were synthesized by traditional solid-state reaction techniques at different reaction temperatures (710-920 ℃) to observe the phase transformation. The phase purity of the resultant solid was confirmed by powder XRD. When the temperature was higher than 740 ℃, pure β-$SrCdB_2O_5$ phase was obtained, and the powder XRD patterns between 710-740 ℃ are shown in Figure 4. When the temperature was 710 ℃, the powder XRD pattern suggests that it is pure α-$SrCdB_2O_5$ phase. Afterwards, the polycrystalline samples which were synthesized at 720 and 730 ℃ were a mixture of α- and β-$SrCdB_2O_5$. When the temperature was raised to 920 ℃, the powders melted. According to the result of solid-state reactions, the phase transformation occurred between 710-740 ℃. (2) The TG-DSC of pure α-$SrCdB_2O_5$ phase was then measured (Figure S2 in the SI). The DSC curve exhibits only one obvious endothermic peak at 921 ℃ upon heating to 1000 ℃. There is no weight loss on the TG curve. This result reaffirms that 921 ℃ is the melting temperature which is consistent with our results of the powder XRD patterns. Furthermore, the powder samples of β-$SrCdB_2O_5$ after melting have been characterized by the powder XRD. Firstly, we prepared two samples of β-$SrCdB_2O_5$, namely Samples 1 and 2. Afterwards, different cooling rates were adopted after the

Samples 1 and 2 melt at 1000 ℃ for 10 h. For Sample 1, the temperature was decreased from 1000 to 800 °C at a rate of 2 °C/h, and allowed to cool to room temperature after the furnace was turned off. Powder XRD of Sample 1 revealed that the product is mainly *β*-$SrCdB_2O_5$ (Figure S3 in the SI). For Sample 2, the melted *β*-$SrCdB_2O_5$ powder was directly quenched in ice-water mixture. Powder XRD pattern of Sample 2 revealed that the main product is a new phase mixed with some $Sr_2B_2O_5$. Subsequently, the new phase was identified as a new polymorph of $Cd_2B_2O_5$. The characterization of the new $Cd_2B_2O_5$ phase is underway and will be published elsewhere.

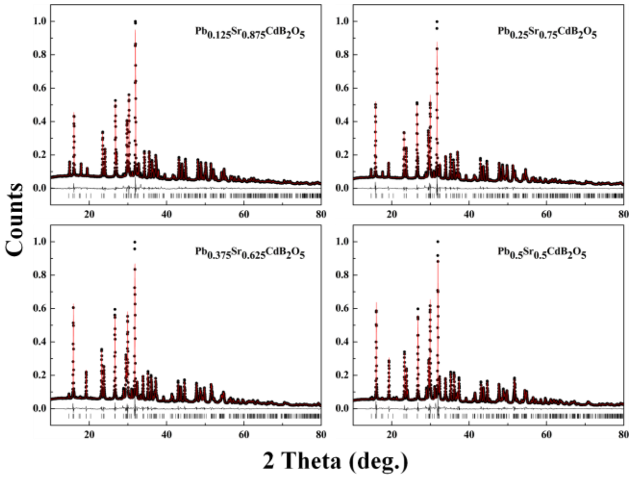

Figure 5. Profile fit to the powder XRD patterns of $Pb_xSr_{1-x}CdB_2O_5$ (x = 0.125, 0.25, 0.375, 0.5). The symbol ● represents the observed value, solid line represents the calculated value; the marks below the diffraction patterns are the calculated reflection positions, and the difference curve is shown at the bottom of the figure.

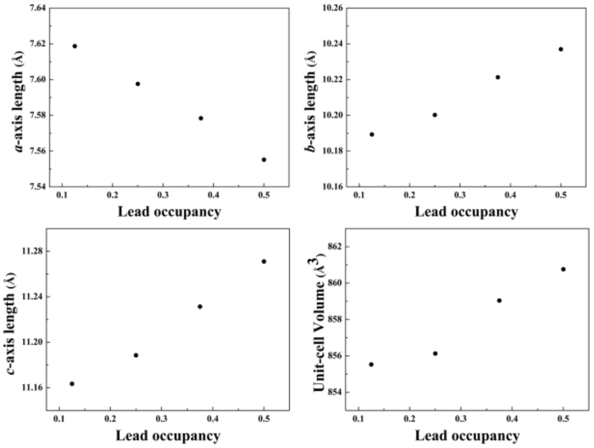

Figure 6. Variation of the lattice parameters as a function of the lead occupancy for $Pb_xSr_{1-x}CdB_2O_5$ (x = 0.125, 0.25, 0.375, 0.5) in the *a*-axis (a), the *b*-axis (b), the *c*-axis (c), and the volume (d).

Furthermore, the total electronic energy calculation was performed for both compounds. As shown in Table S5 in the SI, the calculation based on experimental crystallographic data gives a slightly lower total energy for the high-temperature phase, confirming *β*-$SrCdB_2O_5$ is energetically more favoured. The difference between the two polymorphs is about 2.124 kJ/mol. Therefore, we speculated that the Pb^{2+}-doped compounds, $Pb_xSr_{1-x}CdB_2O_5$, may prefer to adopt the structure type of *β*-$SrCdB_2O_5$ rather than *α*-$SrCdB_2O_5$. Inspired by this viewpoint, we substituted the Sr^{2+} cation for Pb^{2+} up to x = 0.5 successfully to form $Pb_{0.125}Sr_{0.875}CdB_2O_5$, $Pb_{0.25}Sr_{0.75}CdB_2O_5$, $Pb_{0.375}Sr_{0.625}CdB_2O_5$ and $Pb_{0.5}Sr_{0.5}CdB_2O_5$ in this work. The structures of Pb^{2+}-doped compounds were refined with the Rietveld method (Jana2006).[12] The final refinement yielded Rp and Rwp within a reasonable value range. Figure 5 shows the profile fit of the diffraction pattern and the crystallographic data are given in Table 2. As can be seen in Figure 6, the cell volume of $Pb_xSr_{1-x}CdB_2O_5$ increases with an increasing amount of Pb^{2+} on the Sr^{2+} sites. However, the unit cell changes are anisotropic: while the refined unit cell parameters *a* continuously decrease, those of *b* and *c* slightly increase (see Figure 6 and Table 2). When x is higher than 0.5, it can not keep the kind of crystal structure of *β*-$SrCdB_2O_5$ due to the Pb^{2+} volume effect. Moreover, we also obtained the single crystal of $Pb_{0.4}Sr_{0.6}CdB_2O_5$ (see Table 1). As to the reason why Pb^{2+}-doped compound, $Pb_xSr_{1-x}CdB_2O_5$, can adopt the structure of high-temperature phase, Wang's empirical formula[19] gives us some enlightenments:

$$\rho = -0.480\log|\Delta x| + 0.240(\pm 0.030),\quad \rho = (Z_M^* e^2 / R_M)/(Z_{M'}^* e^2 / R_{M'})$$

Here, x, M, M′ and Z^*e^2/R represent electronegativity, the Sr^{2+} cation, the Pb^{2+} cation, and effective ionic potential, respectively. The Sr^{2+} and Pb^{2+} cations can meet the requirements of this empirical formula. The result of this experiment suggests that *β*-$SrCdB_2O_5$ may be more stable than *α*-$SrCdB_2O_5$ and Pb^{2+}-doped can affect the stability of *β*-$SrCdB_2O_5$.

IR absorption spectrum for *β*-$SrCdB_2O_5$ was measured and the result is presented in Figure S4 in the SI. Referring to the literatures,[20] the peaks at 1381, 1215 and 1124 cm^{-1} can be assigned to the asymmetric stretching vibrations of BO_3, while the peaks located at 978 and 804 cm^{-1} are likely to be from the symmetric stretching vibrations of BO_3. The peaks at 744, 696, 611 and 482 cm^{-1} are attributed to bending vibrations. IR spectrum indicates that only BO_3 groups are included in *β*-$SrCdB_2O_5$.

The UV-Vis-NIR diffuse reflectance spectrum for *β*-$SrCdB_2O_5$ is deposited in Figure S5 in the SI. Absorption (K/S) data were calculated from the following Kubelka-Munk function[13]:

$$F(R) = \frac{(1-R)^2}{2R} = \frac{K}{S}$$

R represents the reflectance, *K* the absorption, and S the scattering factor. The minimum in the second-derivative curves of the Kubelka–Munk function are taken as the maximum of the absorption bands. We can observe that the absorption edge of *β*-$SrCdB_2O_5$ is at about 311 nm (i.e. 3.98 eV).

To gain further insights on the electronic structures and optical properties of *β*-$SrCdB_2O_5$, theoretical calculations based on DFT methods were performed.[15] The band structure of *β*-$SrCdB_2O_5$ is shown in Figure S6 in the SI. It can be seen that *β*-$SrCdB_2O_5$ is a direct gap crystal with the value 3.81 eV at G point which is consistent with the experimental value (3.98 eV) well. The total and partial densities of states (DOS and PDOS) are shown in Figure S7 in the SI. The wide region spanning over -20 to -14 eV is from kernel orbitals. One can see that the top of the VB and the bottom of the CB are mainly from the basic boron–oxygen and Cd–O structural units which indicate that the linear optical effects are primarily due to B-O and Cd–O groups.

Conclusion

In summary, an unusual phenomenon that the density of high-temperature phase (β-$SrCdB_2O_5$) is obviously larger than that of the low-temperature phase (α-$SrCdB_2O_5$) has been investigated in detail. In the view of structure chemistry, we explain the reasons of this density phenomenon. We think that the different dihedral angles of B_2O_5 groups in *α*- and β-$SrCdB_2O_5$ result in different Sr-O layers and crystal structures. The direct reason why *α*-$SrCdB_2O_5$ possesses a smaller density than *β*-$SrCdB_2O_5$ is that the distance between the Sr-O layers in *α*-$SrCdB_2O_5$

(6.329 Å) is longer than that in *β*-$SrCdB_2O_5$ (5.497 Å). The phase transformation between *α*- and β-$SrCdB_2O_5$ was investigated by traditional solid-state reaction techniques and TG-DSC measurement. Furthermore, the comparison of total electronic energy between *α*- and β-$SrCdB_2O_5$ motivated us to substitute the Sr^{2+} cation for Pb^{2+} up to $x = 0.5$ successfully and the results suggest that Pb^{2+}-doped can affect the stability of the high-temperature polymorph of $SrCdB_2O_5$. In addition, first-principles electronic structure calculation shows that the calculated band gap of *β*-$SrCdB_2O_5$ is in good agreement with the experimental one estimated from UV-Vis-NIR absorption spectrum.

Acknowledgements

This work is supported by the “Western Light Foundation” Program of Chinese Academy of Sciences (Grant No. XBBS201214), the “National Natural Science Foundation of China” (Grant Nos. U1303392, 51425206, U1129301), 973 Program of China (Grant No. 2014CB648400), the Xinjiang International Science & Technology Cooperation Program (20146001), the Funds for Creative Cross & Cooperation Teams of CAS, the Special Fund for Xinjiang Key Laboratories (Grant No. 2014KL009).

Notes and references

[a] Key Laboratory of Functional Materials and Devices for Special Environments of CAS; Xinjiang Key Laboratory of Electronic Information Materials and Devices; Xinjiang Technical Institute of Physics & Chemistry of CAS, 40-1 South Beijing Road, Urumqi 830011, China. E-mail: wuhp@ms.xjb.ac.cn (Hongping Wu); slpan@ms.xjb.ac.cn (Shilie Pan)

[b] University of Chinese Academy of Sciences, Beijing 100049, China.

Fax: (86)-991-3838957; Tel: (86)-991-3674558.

[c] College of Chemistry and Molecular Engineering, Peking University, Beijing 100871, China

† Electronic Supplementary Information (ESI) available: CSD-428209 for *β*-$SrCdB_2O_5$ Crystal data (CIF file); Checkcif; Atomic coordinates, related anisotropic displacement parameters, the bond valence calculation for all atoms; selected bond lengths (Å) and angles (deg.) for *α*- and *β*-$SrCdB_2O_5$; the magnitudes of dipole moments and total energy calculated for *α*- and *β*-$SrCdB_2O_5$; TG-DSC curves of α-$SrCdB_2O_5$; calculated XRD patterns and the before and after melting XRD patterns of *β*-$SrCdB_2O_5$; the IR spectrum, the UV-Vis-NIR diffuse reflectance spectrum, the band structure and the total and partial densities of states for *β*-$SrCdB_2O_5$. See DOI: 10.1039/b000000x/

1 J. J. Zhang, Z. H. Zhang, W. G. Zhang, Q. X. Zheng, Sun Y. X., C. Q. Zhang, X. T. Tao, *Chem. Mater*. 2011, **23**, 3752; W. G. Zhang, X. T. Tao, C. Q. Zhang, H. J. Zhang, M. H. Jiang, *Cryst. Growth Des.* 2009, **9**, 263.

2 K. M. Ok, P. S. Halasyamani, *Angew.Chem. Int. Ed.* 2004, **43**, 5489; K. M. Ok, P. S. Halasyamani, *Inorg. Chem.* 2005, **44**, 9353.

3 S. R. Vippagunta, H. G. Brittain, D. J. W. Grant, *Adv. Drug. Delivery. Rev*. 2001, **48**, 3; H. G. Brittain, *J. Pharm. Sci*. 2007, **96**, 705.

4 C. T. Chen, Y. C. Wu, A. D. Jiang, B. C. Wu, G. M. You, *Sci. Sin. B* 1985, **28**, 235.

5 S. F. Wu, G. F. Wang, J. L. Xie, X. Q. Wu, Y. F. Zhang, X. Lin, *J. Cryst. Growth* 2002, **245**, 84.

6 M. He, H. Okudera, A. Simon, J. Kohler, S. F. Jin, X. L. Chen, *J. Solid State Chem.* 2013, **197**, 466.

7 *SAINT-Plus*, version 6.02A; Bruker Analytical X-ray Instruments, Inc.: Madison, WI, 2000.

8 G. M. Sheldrick, SHELXTL, version 6.14; Bruker Analytical X-ray Instruments, Inc.: Madison, WI, 2003.

9 G. M. Sheldrick, SHELXS-97, Program for X-ray Crystal Structure Solution; University of Göttingen: Göttingen, Germany, 1997.

10 A. L. Spek, *J. Appl. Crystallogr*. 2003, **36**, 7.

11 N.E. Brese, M. Okeeffe, *Acta Crystallogr.* B 1991, **47**, 192; I. D. Brown, D. Altermatt, *Acta Crystallogr*. B 1985, **41**, 244.

12 V. Petricek, M. Dusek, Palatinus L. *Jana2006 Program*, 2006.

13 P. Kubelka, F. Z. Munk, *Tech. Phys.* 1931, **12**, 593; J. Tauc, *Mater. Res. Bull*. 1970, ***5***, 721.

14 S. J. Clark, M. D. Segall, C. J. Pickard, P. J. Hasnip, M. J. Probert, K. Refson,M. C. Payne, *Z. Kristallogr.* 2005, **220**, 567.

15 D. M. Ceperley, B. J. Alder, *Phys. Rev. Lett.* 1980, **45**, 566; J. P. Perdew, A. Zunger, *Phys. Rev. B* 1981, **23**, 5048.

16 H. J. Monkhorst, J. D. Pack, *Phys. Rev. B* 1976, **13**, 5188.

17 M. H. Lee, Ph.D. Thesis, The University of Cambridge, 1996; J. Lin, A. Qteish, M. Payne and V. Heine, *Phys. Rev. B* 1993, **47**, 4174; A. M. Rappe, K. M. Rabe, E. Kaxiras, J. D. Joannopoulos, *Phys. Rev. B* 1990, **41**, 1227.

18 J. Cao, J. Y. Gao, S. L. Pan, H. W. Yu, W. W. Zhao, Z. H. Yang, *Inorg. Chim. Acta* 2012, **392**, 459.

19 G. F. Wang, *J. Inorg. Mater*. (Chinese) 1991, **6**, 326.

20 Y. Yang, S. L. Pan, J. Han, X. L. Hou, Z. X. Zhou, W. W. Zhao, Z. H. Chen, M. Zhang, *Cryst. Growth Des.* 2011, **11**, 3912; L. Wang, S. L. Pan, L. X. Chang, J. Y. Hu, H. W. Yu, *Inorg. Chem.* 2012, **51** 1852; Y. J. Wang, S. L. Pan, X. L. Tian, Z. X. Zhou, G. Liu, J. Wang, D. Z. Jia, *Inorg. Chem.* 2009, **48**, 7800.

Graphical Abstract

An unusual density evolution between $SrCdB_2O_5$ polymorphs

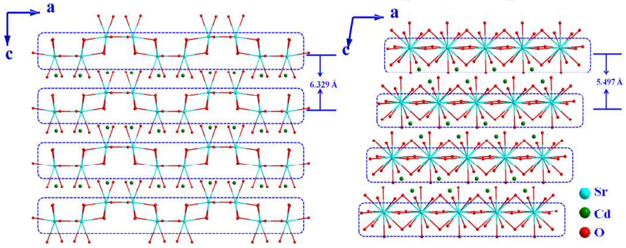

(a) (b)

A new $SrCdB_2O_5$ phase (β- $SrCdB_2O_5$) has been discovered and an unusual phenomenon that the density of high-temperature phase (β-$SrCdB_2O_5$) is obviously larger than that of the low-temperature phase (α-$SrCdB_2O_5$) has been investigated in detail. Furthermore, the Pb^{2+}-doped compounds, $Pb_xSr_{1-x}CdB_2O_5$ (x = 0.125, 0.25, 0.375, 0.5), have also been investigated by powder refinement.